



## RESEARCH ARTICLE

10.1002/2016RS006111

## Key Points:

- Numerical weather prediction supplies 6 h regional rain accumulations
- The distribution of 6 h accumulations can be used to predict 1 min distributions
- Some annual variation is captured in the distribution of 6 h accumulations

## Correspondence to:

K. S. Paulson,  
k.paulson@hull.ac.uk

## Citation:

Paulson, K. S. (2017), Estimating 1 min rain rate distributions from numerical weather prediction, *Radio Sci.*, 52, 176–184, doi:10.1002/2016RS006111.

Received 21 JUN 2016

Accepted 30 DEC 2016

Accepted article online 7 JAN 2017

Published online 26 JAN 2017

## Estimating 1 min rain rate distributions from numerical weather prediction

Kevin S. Paulson<sup>1</sup> 

<sup>1</sup>School of Engineering, University of Hull, Hull, UK

**Abstract** Internationally recognized prognostic models of rain fade on terrestrial and Earth-space EHF links rely fundamentally on distributions of 1 min rain rates. Currently, in Rec. ITU-R P.837-6, these distributions are generated using the Salonen-Poiars Baptista method where 1 min rain rate distributions are estimated from long-term average annual accumulations provided by numerical weather prediction (NWP). This paper investigates an alternative to this method based on the distribution of 6 h accumulations available from the same NWPs. Rain rate fields covering the UK, produced by the Nimrod network of radars, are integrated to estimate the accumulations provided by NWP, and these are linked to distributions of fine-scale rain rates. The proposed method makes better use of the available data. It is verified on 15 NWP regions spanning the UK, and the extension to other regions is discussed.

### 1. Introduction

Rain-induced attenuation is a major impairment for wireless line of sight communications operating above 10 GHz, such as terrestrial and Earth-space links and links to high-altitude platforms and unmanned airborne vehicles. A fundamental input parameter to the International Telecommunication Union Radiocommunication Sector (ITU-R) models of rain fade on terrestrial and Earth-space links, Rec. ITU-R P.530-16 [*International Telecommunication Union*, 2015] and Rec. ITU-R P.618-12 [*International Telecommunication Union*, 2015], respectively, is the 1 min rain rate exceeded for 0.01% of an average year,  $R_{0.01\%}$ . Many parts of the world do not have measured data of 1 min rain rates and so rely upon distributions provided by Rec. ITU-R P.837-6 [*International Telecommunication Union*, 2012]. This recommendation is based on work by Salonen-Poiars Baptista (SPB) [*Salonen and Poiars Baptista*, 1997; *Poiars Baptista and Salonen*, 1998; *International Telecommunication Union Radiocommunication Sector (ITU-R) Study Group 3*, 2012]. It assumes that the average annual 1 min rain rate complementary cumulative distribution function (CCDF or exceedance), globally, is well approximated by a double exponential distribution. This distribution has four parameters. The SPB method links these four parameters to three parameters derived from numerical weather prediction (NWP), specifically ERA40 data provided by the European Centre for Medium-Range Weather Forecasts [*Uppala et al.*, 2005]. The three NWP parameters are long-term average annual accumulations of convective and stratiform precipitations and the proportion of 6 h intervals that contain precipitation, for large regions spanning 1 to 2 degrees of latitude and longitude. The method requires 6 h time series of precipitation accumulation to calculate the proportion containing precipitation but does not otherwise directly use the distribution of the 6 h accumulations.

This paper proposes a new method to predict the distributions of 1 min rain rates from NWP data, as an alternative to the SPB method. The proposed method assumes that over the long term (many years), each regional 6 h accumulation is associated with a distribution of 1 min point rain rates. Once these distributions are known, the distribution of 6 h accumulations can be transformed into the distribution of 1 min rain rates. This paper uses UK Meteorological Office Nimrod composite rain rate images to estimate both regional 6 h accumulations and the 1 min point rain rate distribution. Simultaneous knowledge of these allows the link between them to be explored.

Section 2 presents the SPB method, while section 3 describes the UK Meteorological Office Nimrod data used for this investigation. Section 4 introduces the proposed new method, while sections 5 and 6 present experimental results, based on its application with different levels of approximation, using five regions spanning the UK. Section 7 tests the most practical form of the method on 10 further regions, not used for method development. Conclusions are drawn in section 8.

## 2. The Salonen-Poiaries Baptista Method

The Salonen-Poiaries Baptista (SPB) method provides a method for estimating the 1 min rain rate distribution, globally. The average annual 1 min rain rate CCDF is assumed to have a distribution well described by the double exponential:

$$F(R) = P_0 e^{-aR \frac{1+bR}{1+cR}} \tag{1}$$

for rain rate  $R > 0$ .  $F(R)$  is the probability of experiencing a rain rate greater than  $R$ , and  $P_0$  is the probability of a 1 min interval experiencing rain. The four parameters  $P_0$ ,  $a$ ,  $b$ , and  $c$  control the shape of the distribution and match the distribution to the local climate. At low rain rates, as  $R \rightarrow 0^+$ , equation (1) is exponential with an exponent of  $-aR$ . For large rain rates it is exponential with an exponent  $-(ab/c)R$ . Typically, the exponent is closer to zero for increasing rain rate, and so  $0 < b < c$ . Parameters  $b$  and  $c$  control both the final exponent and where the transition between the two exponential regimes occurs. A disadvantage of equation (1) is that it cannot be analytically integrated to yield rain accumulation. It can be differentiated to yield a complicated probability density function.

Rec. ITU-R P.837-6 uses the SPB method to calculate the four distribution parameters from three regional, long-integration time, rain parameters. The NWP parameters are as follows:

- $M_S$  = the mean annual stratiform rain accumulation (mm).
- $M_C$  = the mean annual convective rain accumulation (mm).
- $P_{r6}$  = the probability of rainy 6 h periods (%).

These parameters are defined over the large regions defined by the NWP system used. The size of the regions affects the interpretation of parameter  $P_{r6}$ , which increases with increasing area. The underlying 6 h rain accumulations typically decrease with increasing area, and integration time, due to the incidence of short-duration rain events smaller than the NWP region. These NWP integration areas are much larger than the convective events that typically determine the rain rates associated with radio system outage.

The Rec. ITU-R P.837-6 model estimates the distribution parameters from these input parameters by using

$$\begin{aligned}
 P_0 &= P_{r6} \cdot \left( 1 - e^{-\alpha_1 \frac{M_S}{P_{r6}}} \right) \\
 b &= \frac{M_C + M_S}{\alpha_2 \times P_0} = \frac{M_T}{\alpha_2 \times P_0} \\
 c &= \alpha_3 \cdot b \\
 a &= \alpha_4
 \end{aligned} \tag{2}$$

The constants have changed with revisions of Rec. ITU-R P.837, and the current values are  $\{\alpha_1, \alpha_2, \alpha_3, \alpha_4\} = \{0.0079, 21797, 26.02, 1.09\}$ . The four SPB distribution parameters are estimated from three NWP parameters, requiring some dependency between them. The method is not self-consistent; i.e., the calculation of the rain accumulation from the SPB distribution does not yield the input  $M_T \equiv M_C + M_S$ , but this is of little importance for radio applications. The SPB method uses a fixed global constant  $a = 1.09$ , describing the distribution of light rain. Also, as  $c$  is a constant times  $b$ , the ratio  $ab/c = \alpha_4/\alpha_3$  is the exponential exponent of the high rain rate tail of the distribution.

The global availability of NWP data, combined with this transformation, yields a globally applicable method to estimate the 1 min rain rate distribution, in particular R0.01%, and hence the rain fade distribution. The SPB method is based on 1.125° gridded ERA40 data with regions with an approximate linear size of 100 km. All three parameters depend upon the integration area and integration time and so are not immediately applicable to other NWP data sets. It is not clear from published sources how the SPB transformation was derived. However, it is consistent with several reasonable heuristics; i.e., regions that experience rain more often will experience more low rain fade, and higher mean rain rates are associated with more extreme fades.

A weakness of the SPB method is the use it makes of the 6 h precipitation time series. These data are required to calculate  $P_{r6}$ , but otherwise, the distribution is lost as these accumulations are summed to yield annual accumulations. Many NWP systems do not yield zero rain accumulations but instead provide a distribution of small values around zero, both positive and negative. The definition of  $P_{r6}$  requires the selection of an

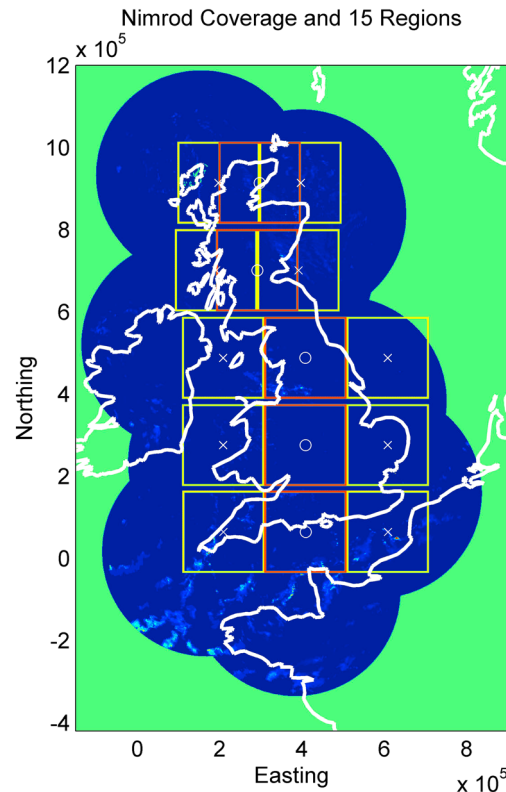


**Figure 1.** Map showing Nimrod composite rain field, the five square regions used to develop the method in this paper (with centers 0), and 10 regions used to test the method (with centers x). The white outline indicates the coast of the UK and nearby countries.

Rain data from 15 regions have been extracted from the Nimrod data set. The five regions used to develop the method are 200 km squares and cover Southern England (SE), the Midlands (ML), Northern England (NE), Southern Scotland (SS), and Northern Scotland (NS). The regions were chosen to correspond to grid cells in the NOAA National Centers for Environmental Prediction/National Center for Atmospheric Research Reanalysis I data set, which provides estimates of accumulations due to precipitation and convective precipitation, over a  $1.875^\circ$  global grid. A further 10 regions of the same size were selected for verification, to the east and west of these regions. Figure 1 illustrates the five regions used for method development.

Rain data from 15 regions have been extracted from the Nimrod data set. The five regions used to develop the method are 200 km squares and cover Southern England (SE), the Midlands (ML), Northern England (NE), Southern Scotland (SS), and Northern Scotland (NS). The regions were chosen to correspond to grid cells in the NOAA National Centers for Environmental Prediction/National Center for Atmospheric Research Reanalysis I data set, which provides estimates of accumulations due to precipitation and convective precipitation, over a  $1.875^\circ$  global grid. A further 10 regions of the same size were selected for verification, to the east and west of these regions. Figure 1 illustrates the five regions used for method development.

#### 4. Introduction to the Proposed Method

In this section a method is developed to estimate point rainfall rate distribution by combining distributions of rainfall rate conditioned to classes of spatially and temporally integrated rain amounts. Regional 6 h accumulations do not capture the fine spatial or temporal resolution required to calculate 1 min point rain rate distributions. A 6 h accumulation could be caused by a long period of wide-spread light rain or a short, localized burst of heavy rain. Each 6 h regional accumulation,  $A$ , will be associated with a long-term exceedance distribution of 1 min point rain rates  $F(R|A)$ . For individual 6 h intervals with accumulation  $A$ , the regional distribution of 1 min rain rates will vary. However, as the number of intervals increases to span many years, the

accumulation threshold, below which accumulations are treated as zero. It is not clear in the literature how this threshold is chosen or its effect on the SPB method. The summing of accumulations loses a lot of information. A wide range of accumulation time series could yield the same annual accumulation and  $P_{r6}$ . That is, accumulation could be uniformly distributed across all wet 6 h intervals or concentrated in a few. This suggests that a more powerful method could be developed if the distribution of accumulations was used.

### 3. Nimrod Data

This section describes the data used to investigate the link between rain distributions at NWP scales and at the 1 min point scale. UK Meteorological Office Nimrod composite rain radar data are the principal data set used. The composite rain rate maps contain near-instantaneous rain rate measurements over integration areas of an approximate diameter of 1 km, spanning the UK and produced every 5 min. Distributions of Nimrod rain rates have been shown to be good estimates of distributions of 1 min rain rates derived from networks of rapid-response rain gauges [Paulson, 2016]. Furthermore, Nimrod data can be integrated, spatially and temporally, to yield the same regional 6 h accumulations as are estimated by NWP systems.

The Nimrod system combines data from a network of 15 C-band radars with satellite data, together with surface reports and numerical weather prediction (NWP) fields. Composite rain field images are produced, with a 5 min sample interval, and presented on a 1 km spatial Cartesian grid, spanning the UK and parts of western Europe. These are available from the British Atmospheric Data Centre from April 2004 to the present. Although presented on a uniform grid, the actual spatial averaging is limited by the distance from a point to the nearest radar. The Nimrod system, radar calibration, and the formation of composite rain field data are described in Harrison *et al.* [2000].

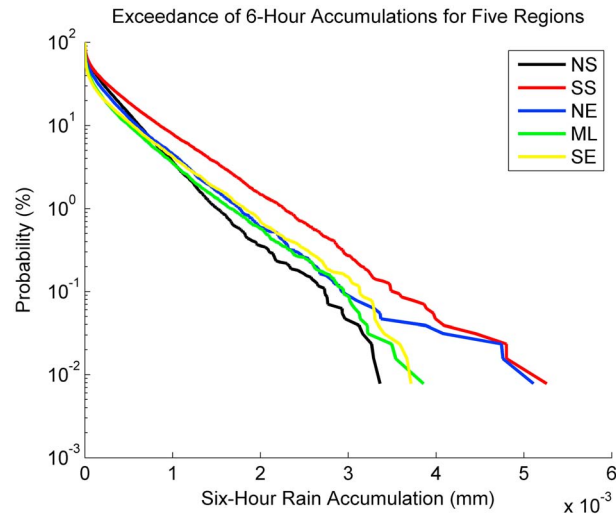


**Figure 2.** Distribution of 6 h accumulations for the five UK regions derived from 10 years of Nimrod data from January 2005 to January 2015.

the underlying fine-scale distribution will be associated with changes in one or both of the distributions  $f_{NWP}(A)$  and  $F(R|A)$ . The distribution  $f_{NWP}(A)$  is readily available from NWP systems and so the assumption that  $F(R|A)$  is fixed yields a first-order estimate of variation in the underlying fine-scale distribution. An example application of this is in the estimation of changes in 1 min distributions due to gradual climate change.

### 5. Testing a Method Based on Measured $F(R|A)$

In this section, we estimate the distributions  $F(R|A)$  from Nimrod data for the five main regions spanning the UK (NS, SS, NE, ML, and SE). We then use these, and Nimrod-derived distributions  $f_{NWP}(A)$ , to estimate annual 1 min rain rate distributions.

For each of the five regions, all Nimrod data from each month from January 2005 to January 2015 are combined to yield exceedance distributions of 1 km accumulations and integrated to yield 6 h regional accumulation time series. Each region yields  $200 \times 200$  rain samples at approximately 1 km resolution, in the Nimrod map produced every 5 min. A month typically yields  $30 \times 24 \times 12$  maps and so a total of  $346 \times 10^6$  fine-scale rain samples. A

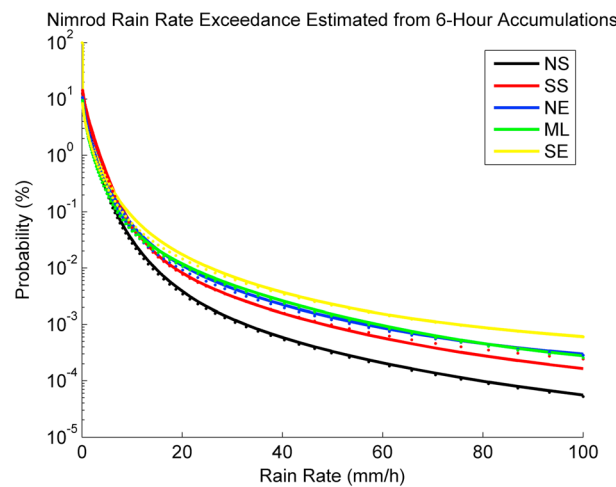


**Figure 3.** Rain rate exceedance distributions for the five UK regions derived from 10 years of data from January 2005 to January 2015. The dotted lines are the measured distributions, while the solid lines are the estimates derived from 6 h accumulations.

conditional distribution of 1 min rain rates will converge to an average distribution. The average annual distribution will be estimated by using

$$F(R) = \int_0^{\infty} f_{NWP}(A)F(R|A)dA \quad (3)$$

$$\cong \frac{1}{N} \sum_{i=1}^N F(R|A_i)$$

where  $f_{NWP}(A)$  is the probability density function of the NWP accumulation  $A$ . When using NWP data yielding  $N$  regional 6 h accumulations  $A_i$ , the summation can be used. The conditional distributions  $F(R|A)$  depend upon the regional mix of precipitation types and intensities, and so will depend upon climate. A large amount of data are required to estimate these distributions. The distributions  $F(R|A)$  are expected to vary smoothly with  $A > 0$ . Spatial or temporal variation in

the underlying fine-scale distribution will be associated with changes in one or both of the distributions  $f_{NWP}(A)$  and  $F(R|A)$ . The distribution  $f_{NWP}(A)$  is readily available from NWP systems and so the assumption that  $F(R|A)$  is fixed yields a first-order estimate of variation in the underlying fine-scale distribution. An example application of this is in the estimation of changes in 1 min distributions due to gradual climate change.

month will yield  $30 \times 4 = 120$  six-hour accumulations for each region. Figures 2 and 3 illustrate the average annual exceedance distributions for these two precipitation accumulation parameters, derived from all 10 years of Nimrod data. Figure 2 shows near-exponential distributions of 6 h regional accumulations with increasing variability at larger accumulations due to the small number of these events. Southern Scotland (SS) includes two consecutive 6 h accumulations nearly twice as large as any others experienced in 10 years. These correspond to a wide-spread, intense, and slow-moving event on 8 December 2008. This event is likely to have a return time of many decades and not only dominates the statistics for SS but also affects NS and NE. Figure 3 illustrates the regional average annual distribution of Nimrod rain rates, which are a good

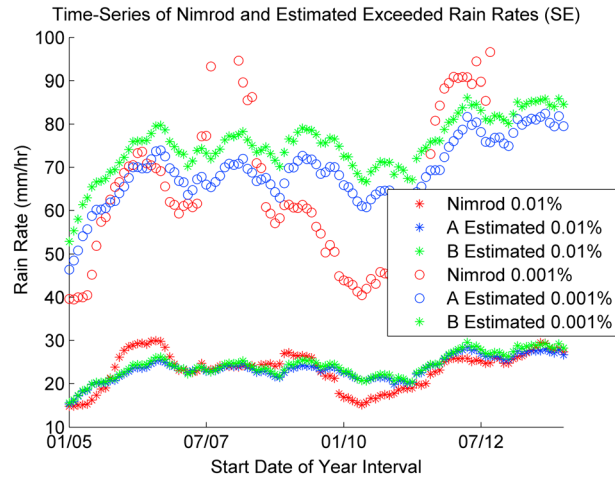


**Figure 4.** Time series of annual exceeded rain rates for the SE region, measured directly from Nimrod, from 6 h accumulations by using measured condition distributions (A) and using fitted conditional distributions (B).

For each accumulation bin, the exceedance distribution of 1 km Nimrod rain rates was calculated for all the samples in the Nimrod rain maps for a region, where the 6 h accumulation lay within that bin range. The average annual distributions were then estimated from the 6 h accumulations using equation (3); i.e., each 6 h accumulation  $A$  was associated with a conditional distribution  $F(R|A)$  estimated by interpolation between the distributions associated with accumulation bin centers. Figure 3 also plots the resulting distributions. Down to an exceedance probability of 0.001%, the predicted and measured distributions are indistinguishable. The root-mean-square differences between measured and estimated rain rates, across the five regions, with exceedances of 0.01% and 0.001%, are 1.1 and 1.7 mm/h, respectively. At lower probabilities more deviation occurs due to the coarseness of the accumulation binning and interpolation processes, particularly for SS where the distribution is strongly determined by one very extreme event.

This numerical experiment is an “inverse crime” as the method is tested against the data used to train the method. However, it demonstrates that the underlying principles are sound and sets an upper limit to the accuracy that could be achieved. A stronger test uses the same method to determine the accuracy of estimates of rain rates exceeded in individual years.

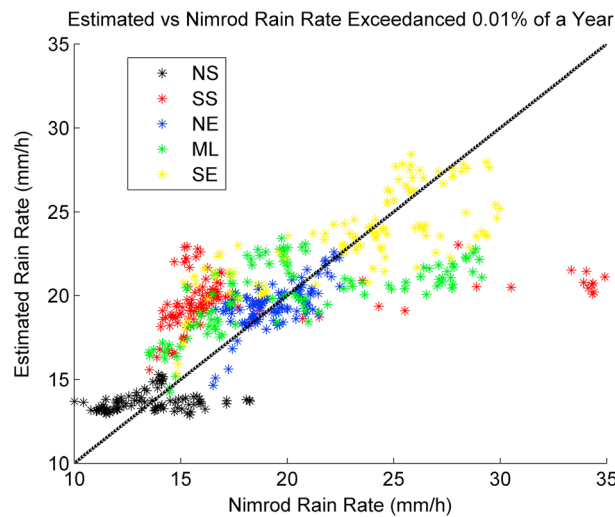


**Figure 5.** Scatterplot of annual 0.01% exceeded rain rates for the five regions, measured directly from Nimrod and estimated from 6 h accumulations, for the period of 2005–2015. The black line indicates equality. Outliers in the SS data are due to the extreme event in 2008.

estimate of 1 min point rain rates. Regional averaging has smoothed away much of the point-to-point variability, but even with 10 years of data, some year-to-year variabilities will remain. Due to the large number of Nimrod samples in a year, the exceedance can be estimated down to very small time percentages.

An initial test of the proposed method was performed by using measured distributions  $F(R|A)$ . Six-hour regional accumulations were allocated to 20 equiprobable bins with near-logarithmically distributed bin boundaries: 0, 0.0008, 0.0036, 0.0086, 0.0153, 0.025, 0.0412, 0.0673, 0.11, 0.17, 0.26, 0.367, 0.52, 0.686, 0.94, 1.286, 1.8, 2.52, 3.6, 14.76, and infinity millimeters. The conditional exceedance  $F(R|A)$  was calculated for each region and for each accumulation bin.

For each accumulation bin, the exceedance distribution of 1 km Nimrod rain rates was calculated for all the samples in the Nimrod rain maps for a region, where the 6 h accumulation lay within that bin range. The average annual distributions were then estimated from the 6 h accumulations using equation (3); i.e., each 6 h accumulation  $A$  was associated with a conditional distribution  $F(R|A)$  estimated by interpolation between the distributions associated with accumulation bin centers. Figure 3 also plots the resulting distributions. Down to an exceedance probability of 0.001%, the predicted and measured distributions are indistinguishable. The root-mean-square differences between measured and estimated rain rates, across the five regions, with exceedances of 0.01% and 0.001%, are 1.1 and 1.7 mm/h, respectively. At lower probabilities more deviation occurs due to the coarseness of the accumulation binning and interpolation processes, particularly for SS where the distribution is strongly determined by one very extreme event.

The distributions  $F(R|A)$  derived from all 10 years are used, but the accumulations measured over the specific year of interest are used to estimate fine-scale exceedance distribution. More error is expected in this case as  $F(R|A)$  experienced in a specific year will be different to the 10 year average. Figure 4 compares the time series of annual 0.01% and 0.001% exceeded rain rates, for SE region, derived directly from distributions of 1 km Nimrod data, with estimates derived by using the 6 h accumulations and the 10 year average  $F(R|A)$ . All 12 month intervals starting on month boundaries are considered. Figure 5 presents the same data, for all five regions, on a scatterplot.

Both plots suggest that the method yields a useful estimate at both probability levels. The Nimrod data exhibit greater variability

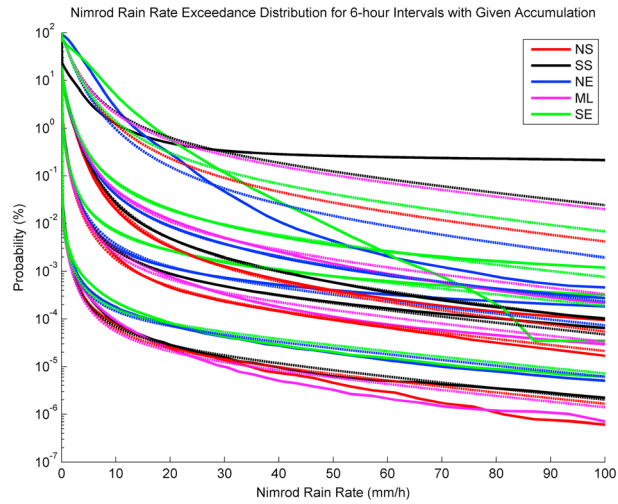


**Figure 6.** Conditional CCDF distributions of 1 km Nimrod rain rates given regional accumulation for the five UK regions. The accumulations are increasing from the bottom to the top group of curves. Measured distributions (solid lines) and fitted distributions (dashed lines).

than the estimates due to the year-to-year variation in  $F(R|A)$ , and this is why the points in Figure 5 are scattered horizontally. However, gross trends are followed, suggesting that the method could be used to predict the performance of radio systems in a climate change scenario by using inputs from weather generators such as the Environment Agency Rainfall and Weather Impacts Generator [Kilsby *et al.*, 2007].

### 6. Testing a Method Based on Model $F(R|A)$

The examples given so far are artificial in that the distributions  $F(R|A)$  are measured from the data. The method would be considerably more useful if these distributions could be generated without accessing large amounts of (or any) rain radar data. Figure 6 illustrates the distributions  $F(R|A)$  for the five regions, for a range of accumulations from dry to very wet periods. Figure 7 shows the same data for the SE region for the 20 accumulations forming equiprobable bins. The major difference between the exceedance distributions for different 6 h accumulations is the probability of rain, i.e., the SPB parameter  $P_0$ . There is also a trend for increasing proportions of heavier rain rates for higher accumulations. The distributions for the very largest accumulations exhibit considerable variation due to the very small number of these accumulations for some regions.

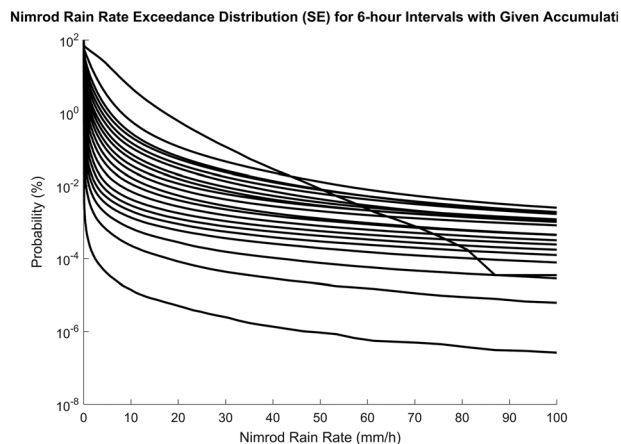


**Figure 7.** Condition CCDF distributions of 1 km Nimrod rain rates given regional accumulation for the Southern England region. The accumulations are increasing from very dry to very wet, from the bottom to the top curve.

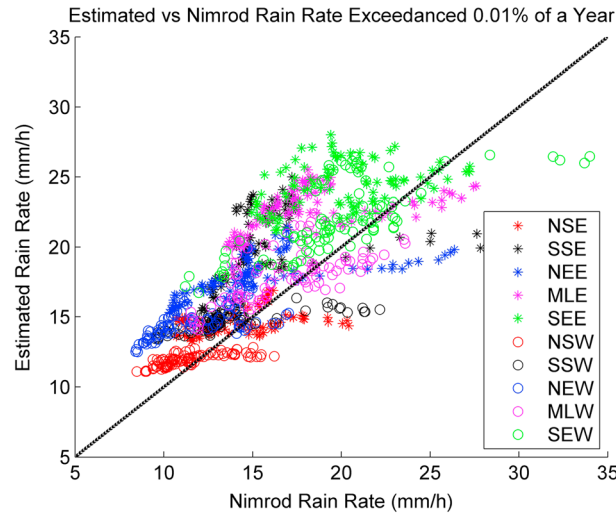


**Figure 8.** Scatterplot of annual 0.01% exceeded rain rates for the 10 regions, measured directly from Nimrod and estimated from 6 h regional accumulations and  $F(R|A)$  from the original five regions, for the period of 2005–2015. The black line indicates equality.

In this section, the data in plots in Figures 6 and 7 are used to derive expressions for approximations to the exceedance distributions  $F(R|A)$ . The SPB double exponential distribution is used, but it is rewritten in a form where the three distribution shape parameters are all rain rates with physical interpretations:

$$F(R) = P_0 \exp\left(-\left(\frac{1}{R_L} \frac{R_0}{R_0 + R} + \frac{1}{R_H} \frac{R}{R_0 + R}\right)R\right) \quad (4)$$

At the light and heavy rain rate extremes, the distribution approaches the exponentials  $\exp(-R/R_L)$  and  $\exp(-R/R_H)$ , respectively. The rain rate  $R_0$  determines where the transition between the two regimes occurs. After considerable numerical experimentation, the following expressions

were found to provide useful descriptions of the variation of the four parameters with 6 h accumulation in millimeters:

$$\begin{aligned} P_0 &= \min(80000A, 100) \\ R_L &= \begin{cases} 0.5 & A < 10^{-7} \\ 3.2 + 1.06\log_{10}(A) + 0.1\log_{10}(A)^2 & \text{else} \end{cases} \\ R_H &= 40 \\ R_0 &= \max(4, 1 + \beta_1 \sqrt{A}) \end{aligned} \quad (5)$$

The parameter  $\beta_1$  depends upon the region, with a strong north-south trend, as it determines the mix of light and heavy rain leading to a given accumulation. From north to south it has the values of 365, 325, 289, 262, and 238. Over the UK the  $\beta_1$ -latitude (Lat) relationship is closely fitted by the expression  $\beta_1 \cong 0.8\text{Lat}^2 - 70\text{Lat} + 1737$ .

Figure 4 plots the annual 0.01% exceeded rain rate calculated by using equation (3) and the fitted conditional distributions (equation (5)), as B estimates. The results are very similar to those calculated by using the 10 year measured average conditional distributions, and so equations (3) and (5) provide a useful method to estimate 1 min rain rates, at outage probabilities, from NWP data.

### 7. Testing on Different Regions

The method based on equations (3) and (5) has been tested by using 10 new regions. These are labeled \*W and \*E and are situated with centers 100 km west and east of NS and SS and 200 km west and east for NE, ML, and SE. These shifts have been constrained by the area covered by the Nimrod composite rain rate data, and the region MLE includes a small area outside of Nimrod coverage. The English regions

**Table 1.** Absolute Percentage Error When Estimating the 10 Year Nimrod 0.01% Exceeded Rain Rate for the 10 Regions not Used to Train the Model, Using Equation (3) and the Measured  $F(R|A)$ , or the Fits Provided by Equation (5)<sup>a</sup>

Region	NSE	SSE	NEE	MLE	SEE	NSW	SSW	NEW	MLW	SEW
Nimrod	15.2	17.3	15.2	18.3	20.1	11.4	13.2	12.9	17.3	20.9
Measured $F(R A)$	14.7 (3.3%)	20.8 (20%)	18.1 (19%)	22.6 (23%)	24.2 (20%)	11.9 (4.7%)	14.6 (11%)	14.8 (15%)	18.0 (3.9%)	22.3 (6.8%)
Fitted $F(R A)$	13.4 (11%)	15.8 (8.7%)	16.0 (5.4%)	19.5 (6.8%)	21.3 (6.4%)	11.8 (3.8%)	13.7 (3.9%)	13.9 (8.1%)	16.4 (5.1%)	20.2 (3.3%)

<sup>a</sup>The rain rates are in mm/h, while the errors in brackets are percentages.

lie adjacent to, and disjoint from, the original five regions, while the Scottish regions overlap by half their area. These areas cover large areas of sea, and so the Nimrod system does not have as much calibration gauge data as for the five regions.

The 10 years of Nimrod data have been examined and the annual distributions of 1 km Nimrod rain rates calculated, along with the 6 h accumulations. For each region, the 10 year average annual distribution of Nimrod 1 km rain rates is estimated by using the 6 h accumulations  $f_{NWP}(A)$ . Two conditional distributions  $F(R|A)$  are tested: those measured on the initial region at the same latitude and those from equation (5) using the parameter  $\beta_1$  from the same latitude. Typically, the difference between Nimrod and predicted CCDF increases as time percentage decreases due to the greater uncertainty and interannual variability in high rain rates. Figure 8 illustrates the scatterplot of Nimrod 0.01% exceeded rain rates and those estimated by using measured  $F(R|A)$ . Table 1 lists the estimation errors by using both the measured and fitted distributions, when the 10 year average 0.01% exceeded rain rate is estimated. It is notable that the fitted  $F(R|A)$  distributions yield more accurate estimates of average annual R0.01%, indicating that the smoothing across regions has yielded better estimates of the long-term  $F(R|A)$  than is provided by the measurements from a single region. The errors in Table 1 can be compared to the best fit reported between the SPB method and measurements on the DBSG3 database, yielding an RMS error of 30% [Castanet et al., 2007].

## 8. Conclusions

The SPB method, which underpins Rec. ITU-R P.837, does not make the best use of its input data. It requires time series of 6 h regional precipitation accumulations to estimate  $P_{r6}$  but then integrates to annual accumulations. The annual distributions of accumulations contain information of year-to-year variability. Assuming that the mix of event types is the same in each year allows a first-order approximation of the 1 min rain rate distribution to be estimated from the distribution of 6 h regional accumulations. The estimate exhibits less year-to-year variability due to this assumption. However, it is adequate for estimation of average annual distributions and is almost certainly applicable to the tracking of long-term trends.

A weakness of the method as it stands is the dependence upon the parameter  $\beta_1$ . This parameter controls where the double exponential distributions  $F(R|A)$  transition from the first to the second exponent and is linked to the mix of rain event types. This parameter has shown monotonic dependence on latitude in this study restricted to the UK. This gross feature is expected to continue to other latitudes due to the link between solar forcing and convective rain. However, variation is also to be expected with topography, e.g., orographic rainfall associated with mountain ranges. Both this method and the SPB method are expected to be less accurate in areas that experience a sizable proportion of solid or mixed phase hydrometeors, i.e., higher latitudes or altitudes. These areas also experience the weakest link between precipitation distributions and fade distributions.

This work has focused on the UK due to the availability of fine-scale composite rain maps. Future work will test the method in other climates, particularly in the tropics, in an attempt to produce global maps of  $\beta_1$ . Predictions based on the method will be tested against the database of ITU-R Study Group 3: DBSG3. The method has been shown to work very well over the five regions that span the UK. Weather simulators will be used to predict trends in outage rain rates in the UK over the next few decades given International Panel on Climate Change Representative Concentration Pathways [Moss et al., 2008]. Combined with the models of interannual variability developed in Jeannin et al. [2013] and Boulanger et al. [2013], the method developed in this paper can contribute to the evolution of ITU-R Rec. 837.

### Acknowledgments

This work was not funded and made use of Nimrod composite rain maps produced by the UK Meteorological Office and supplied by the British Atmospheric Data Centre: Met Office (2003): Meteorological Office Rain Radar data from the NIMROD system. NCAS British Atmospheric Data Centre, March 2015: <http://catalogue.ceda.ac.uk/uuid/82adec1f896af6169112d09cc1174499>.

### References

- Boulanger, X., N. Jeannin, L. Féral, L. Castanet, F. Lacoste, and F. Carvalho (2013), Inter-annual variability, risk and confidence intervals associated with propagation statistics. Part II: Parameterization and applications, *Int. J. Satell. Commun. Network.*, 32(5), 423–441, doi:10.1002/sat.1059.
- Castanet, L., C. Capsoni, G. Blarmino, D. Ferrado, and A. Martellucci (2007), Development of a new global rainfall model based on ERA40 TRMM and GPCP products, Proc. ISAQP07, Niigata, Japan, 1378–1381.
- Harrison, D. L., S. J. Driscoll, and M. Kitchen (2000), Improving precipitation estimates from weather radar using quality control and correction techniques, *Meteorol. Appl.*, 6, 135–144.
- International Telecommunication Union (2012), *Characteristics of precipitation for propagation modelling ITU-R Recomm.*, pp. 837–6, Geneva, Switzerland.

- International Telecommunication Union (2015), *Propagation data and prediction methods required for the design of terrestrial line-of-sight systems ITU-R Recomm*, pp. 530-16, Geneva, Switzerland.
- International Telecommunication Union (2015), *Propagation data and prediction methods required for the design of Earth-space telecommunication systems ITU-R Recomm*, pp. 618-12, Geneva, Switzerland.
- Jeannin, N., X. Boulanger, L. Féral, L. Castanet, and F. Lacoste (2013), Inter-annual variability, risk and confidence intervals associated with propagation statistics. Part I: Theory of estimation, *Int. J. Satell. Commun. Network.*, 32(5), 407–421, doi:10.1002/sat.1060.
- Kilsby, C. G., P. D. Jones, A. Burton, A. C. Ford, H. J. Fowler, C. Harpham, P. James, A. Smith, and R. L. Wilby (2007), A daily weather generator for use in climate change studies, *Environ. Modell. Software*, 22, 1705–1719.
- Moss, R., et al. (2008), *Towards New Scenarios for Analysis of Emissions, Climate Change, Impacts, and Response Strategies*, 132 pp., Intergovernmental Panel on Clim. Change, Geneva, Switzerland.
- Paulson, K. (2016), Evidence of trends in rain event size effecting trends in rain fade, *Radio Sci.*, 51, 142–149, doi:10.1002/2015RS005832.
- Poiars Baptista, J. P. V., and E. T. Salonen (1998), Review of rainfall rate modelling and mapping Proc. of URSI Commission F Open Symposium on Climatic Parameters in Radiowave Propagation Prediction (CLIMPARA'98), Ottawa, Ontario, Canada.
- Salonen, E. T., and J. P. V. Poiars Baptista (1997), A new global rainfall rate model, 10th International Conference on Antennas and Propagation, 14–17 April 1997, Conference Publication No. 436 0 IEE.
- Uppala, S. M., et al. (2005), The ERA-40 re-analysis, *Q. J. R. Meteorol. Soc.*, 131, 2961–3012, doi:10.1256/qj.04.176.